JOURNAL OF SOLID STATE CHEMISTRY 16, 129–139 (1976)

Study by Electron Microscopy and Electron Diffraction of Formation of Nickel Epitaxially Grown Catalysts

GISÈLE DALMAI-IMELIK, CHRISTIANE LECLERCQ, AND ANA MAUBERT-MUGUET*

Centre National de la Recherche Scientifique, Institut de Recherches sur la Catalyse, 39 Boulevard du 11 Novembre 1918, 69626-Villeurbanne, France

Received February 11, 1975; revised, May 20, 1975

In order to study the influence of the crystallographic arrangement at the surface of a metal-supported catalyst on its catalytic properties, catalysts have been prepared with well faceted nickel crystallites presenting particular faces at their surface.

Catalysts were obtained by reduction by hydrogen of nickel antigorite evacuated at different temperatures. The morphology and structure of nickel antigorite, the parent of the catalyst, has been determined by electron microscopy and electron diffraction at different temperatures. Rolled or flat sheets were observed. The texture of the catalysts obtained after reduction was determined. The crystallites of nickel are hexagonal platelets with either their (111) or their (110) plane parallel to the sheet support, depending on the conditions of preparation and reduction. Study of the orientations of (111) type or (110) type was done.

Introduction

The heterogeneity of the surface of a catalyst can play a role in catalysis. This heterogeneity can be connected with the different crystallographic planes at the surface, lattice defects, etc. Many results obtained on films and single crystals have shown that certain crystallographic faces can have a different activity for some reactions. Ertl showed different activation energies for the oxidation of CO, depending on the exposed faces (*1*). Dalmai-Imelik et al. observed that faces (111) and (110) are more active for the reaction of hydrogenation of ethylene than the (100) one and that the chemisorption of hydrocarbons is different on the three faces (*2*, *3*). Cunningham and Gwathmey had found the same result (*4*, *5*) and, moreover, that the (321) face is more active than the (100) face. Lang, Joyner, and Somorjai observed that the dehydrocyclization of the *n*-heptane is different on steps surfaces and on low-indice faces (*6*). Otherwise, the influence of lattice defects on catalytic activity is controverted (*7*).

According to the nature of the support and the method of preparation of metal-supported catalysts, thermodynamic equilibrium of the metallic particles can be modified in such a way that the nature of exposed faces and the ratio of particular atoms with different coordination numbers (corner, edge, or face atoms) can be changed (*8*, *9*, *10*, *11*).

In order to study the influence of crystalline faces nature on the catalytic activity, supported catalysts have been prepared with well-faceted nickel crystallites presenting particular faces at their surface. We have studied the formation of nickel crystallites and the texture and structure of the catalysts obtained by electron microscopy and electron diffraction.

* Present address: Universidad Autonoma Metropolitana, Mexico, D. F., Mexico.

Materials and Experimental Techniques

I. Materials

The catalysts were obtained by reduction by hydrogen of nickel antigorite evacuated at different temperatures. The nickel antigorite has been prepared by stoichiometric mixture of very pure nickel hydroxide (*12*) (without Na ions) and silica (*13*). This silica has been prepared in a plasma flame, and its specific surface is 230 m^2/g. The mixture is heated with water at 300°C for 120 hr in an autoclave, then it is dried at 120°C.

II. Techniques

The experiments were done with a JEM 100B electron microscope, fitted with a goniometer. Its resolving power is 3.5 Å. The preparation of the sample for electron microscopic examination was done by three methods: dispersion in a liquid by ultrasons, single stage carbon replica, or thin sections after embedding in Epon (*14*).

Results

I. Morphology and Structure of Nickel Antigorite

Nickel antigorite is a basic silicate of nickel which can be found in nature. The solid is formed by elementary sheets of about 7 Å of thickness with a tetrahedral and an octahedral layer. Antigorite crystallizes in a monoclinic (*15*) or an orthorhombic system (*16*). We have represented in Figs. 1 and 2 projections of nickel antigorite atoms on (A, B) and (B, C) planes in the case of an orthorhombic structure. The sheets can be flat or rolled in tubes (*17*). According to different authors, these morphologies are connected with the chemical composition of the antigorite and with the difference between the tetrahedral and octahedral layers. Indeed, depending on the amount of silica, we have obtained rolled (Fig. 3) or flat (Fig. 4) sheets. Flat sheets correspond to mixtures with a shortage of silica stoichiometry.

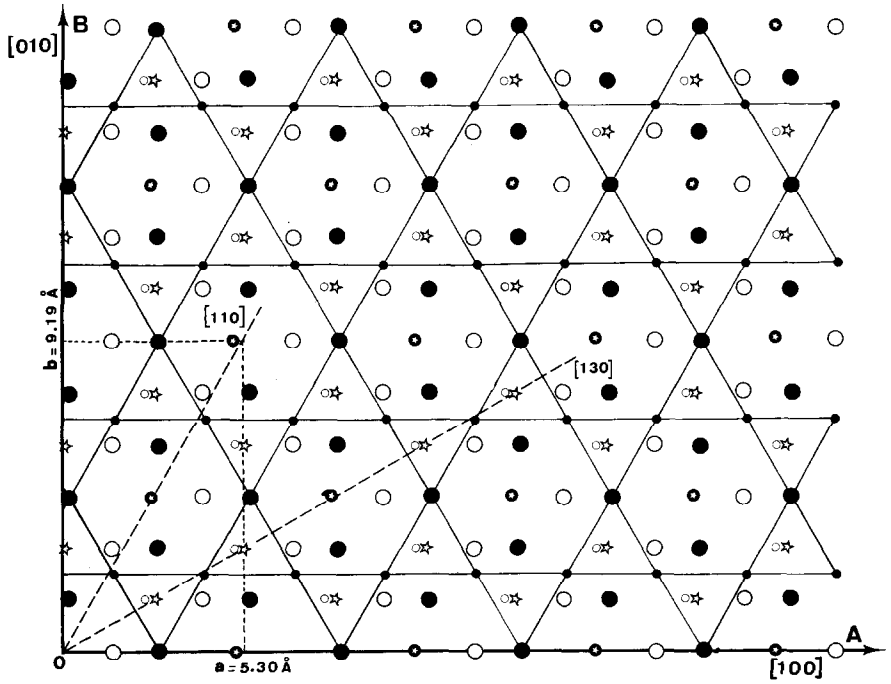

FIG. 1. Projections of nickel antigorite atoms on (A, B) plane.

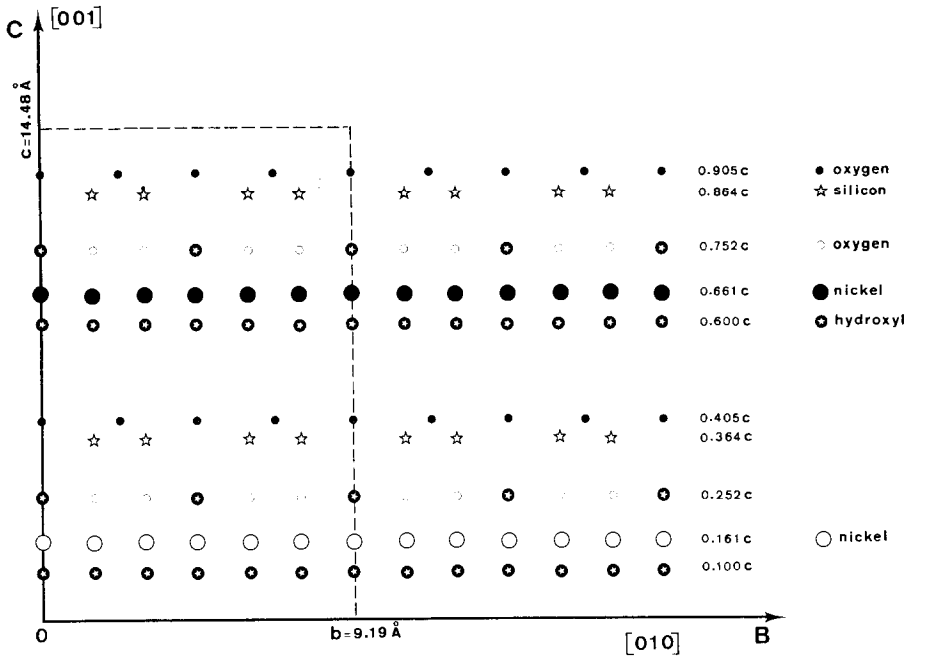

FIG. 2. Projections of nickel antigorite atoms on (B, C) plane.

The nickel antigorites obtained are well crystallized. The X-ray diffraction lines are similar to those in (*18*, *13*) (Table I). From these lines, it can be deduced that our nickel antigorites crystallize in the face-centered orthorhombic system because only the crystallographic planes where $(h + k)$ is even are visible. We obtained extinctions for $(h + k) = 2n + 1$. The calculated parameters are $a = 5.30$ Å, $b = 9.19$ Å, and $c = 7.24$ Å. By electron diffraction on each flat sheet perpendicular to the electron beam, a pattern is obtained corresponding to the [001] projection where only the $hk0$ spots appear. Values of a and b are 5.32 Å and 9.17 Å (Fig. 5). When the sheets are rolled, we observed a streaked pattern (Fig. 6). The value of parameter c can be deduced in this case ($c = 7.24$ Å), and it is observed that the sheets are rolled around the a axis.

II. Heat Treatment of Nickel Antigorite

During heating of nickel antigorite under vacuum, water is desorbed. At 700°C, all the water is lost (*18*). No important variation of morphology and structure is observed by electron microscopy and diffraction below this temperature. Only the a and b parameters become smaller (–4.15%); the axes are conserved.

For higher temperatures a decomposition in NiO occurs. At 960°C, cracks formed by small particles are observed on the sheets. However, the electron diffraction pattern corresponds to a NiO single crystal with its (111) plane perpendicular to the electron beam. In this case, a mosaic structure is observed with all small crystallites oriented by topotaxy from the nickel antigorite support, with the (111) plane parallel to the (001) plane of antigorite and perpendicular to the electron beam.

III. Reduction of Nickel Antigorite Evacuated at Different Temperatures

Nickel antigorite was reduced for 16 hr under 200 torr of hydrogen in a static system. The desorbed water was trapped in a N_2 liquid trap.

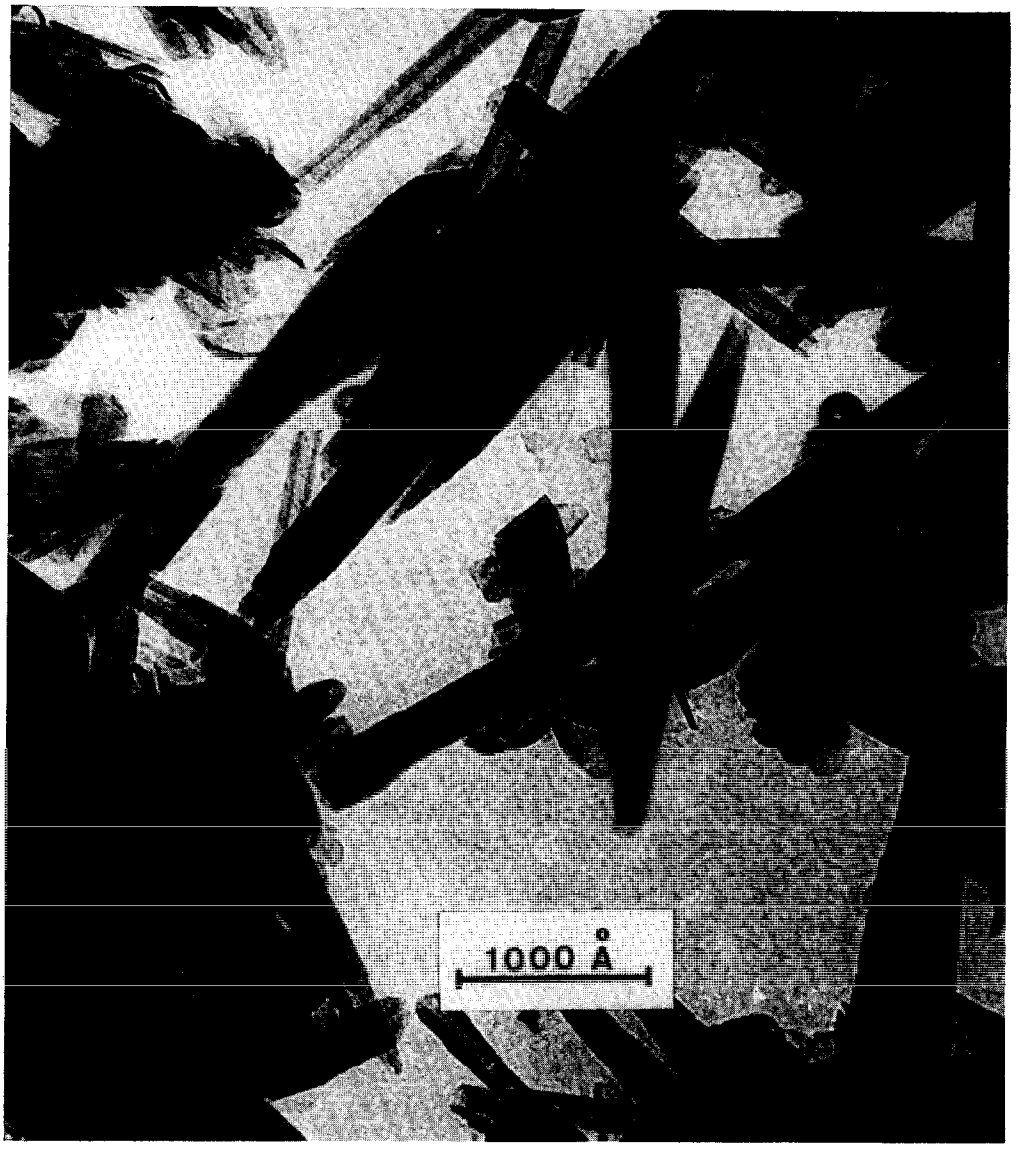

FIG. 3. Nickel antigorite with rolled sheets. ×250,000.

(*1*) *Reduction of nickel antigorite without preliminary heat treatment* (*A 25–700° sample*). The percentage of reduction of the sample increased with the temperature of reduction (*16*). At 700°C the reduction is almost complete (more than 99%). The amount of nickel is 45% by weight. By electron microscopy, we observed nickel crystallites on silica sheets. The form of observed nickel particles is not well defined, and their size is not homogeneous (50 to 250 Å). However, small facets can be seen. By electron diffraction, it was seen that these nickel crystallites are oriented; different electron diffraction patterns were obtained depending on the place in the sample, some patterns corresponding to the (111) nickel planes

FIG. 4. Nickel antigorite with flat sheets. ×180,000.

perpendicular to the electron beam, others to (110) nickel planes, or to a mixture of both orientations. Some patterns with twelve spots on the (220) ring were also observed. When the matter is rolled sheets, only the (110) orientation was observed.

TABLE I

OBSERVED VALUES OF X-RAY AND ELECTRON DIFFRACTION LINES OF NICKEL ANTIGORITE

Present study				Longuet-Escard (*18*)	Martin (*13*)	
X-ray diffraction		Electron diffraction				
d (Å)	$h\,k\,l$	d (Å) (±1%)	$h\,k\,l$	d (Å)	d (Å)	$h\,k\,l$
7.248	0 0 1			7.35	7.23	0 0 1
4.595	0 2 0	4.59	0 2 0 1 1 0	4.52	4.57	0 2 0 1 1 0
3.615	0 0 2			3.58	3.615	0 0 2
2.649	1 3 0 2 0 0	2.65	1 3 0 2 0 0	2.65	2.645	1 3 0 2 0 0
2.492	2 0 1			2.51	2.495	2 0 1
2.33	2 2 0	2.30	2 2 0			
2.139	1 1 3 0 2 3			2.16	2.15	1 1 3 0 2 3
		1.72	3 1 0	1.72	1.725	3 1 0 3 0 1
1.533	0 6 0 3 3 0	1.53	0 6 0 3 3 0	1.52	1.525	0 6 0 3 3 0
1.502		1.32	4 0 0	1.30	1.310	4 0 0

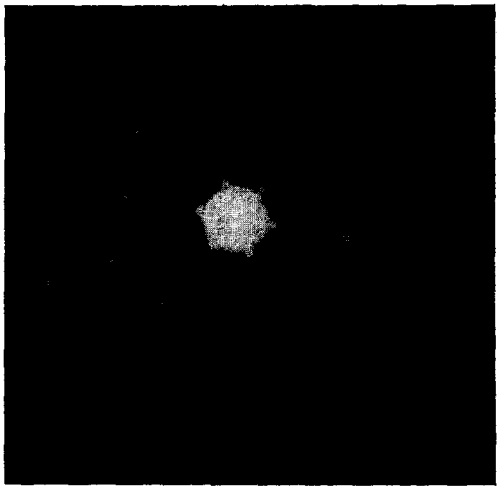

FIG. 5. Electron diffraction pattern obtained on a flat sheet of nickel antigorite.

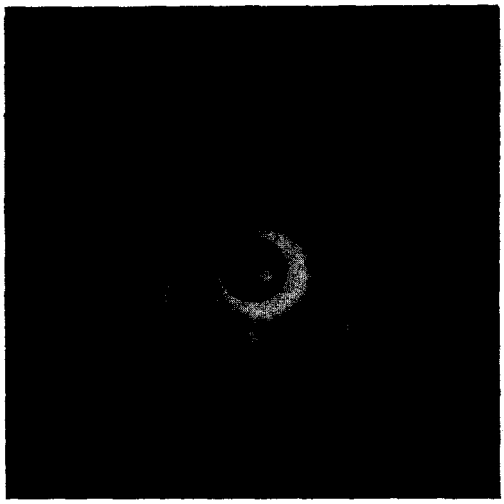

FIG. 6. Electron diffraction pattern obtained on a rolled sheet of nickel antigorite.

(*2*) *Reduction of nickel antigorite evacuated at 700°C.* We have observed samples after reduction by hydrogen at 410, 530, and 700°C for 16 hr (samples, A 700–410°, A 700–530°, A 700–700°).

At 410°C (A 700–410°), some small crystallites of nickel begin to appear at 35% reduction. At 530°C (A 700–530°), the reduction attains 60% and small crystallites (30 to 100 Å)

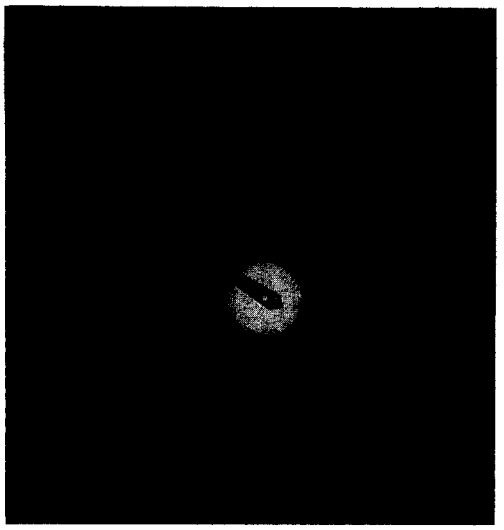

FIG. 7. Electron diffraction pattern obtained on A 700–530° sample.

are observed. An (111) orientation is obtained and the epitaxy of nickel (A spots) on heated nickel antigorite (B spots) can be seen in the diffraction pattern (Fig. 7).

At 700°C (A 700–700°), the reduction is almost complete (more than 99%). Nickel particles are observed on the silica sheet. The form of these particles observed by electron microscopy is hexagonal and their edges are parallel to three directions at 120° (Fig. 8).

The electron diffraction pattern obtained is the same as that in the case of a nickel single crystal with its (111) Ni plane perpendicular to the electron beam.

Dark field images were formed with the electrons corresponding to each of 220 diffraction spots. On these images, most hexagonal crystallites are visible, so it means that they have their (111) planes parallel to the support. Their principal directions are rotated 120°, and it can be observed that few particles are twinned.

Moreover, transversal thin sections of the sheets were done, and it was observed that a part of the nickel crystallites is embedded in the silica sheet. The thickness of these particles is around 40 Å, and two edges are parallel to the plane of the silica sheet. A carbon replica of the surface has shown that flat nickel crystallites are formed on the surface, the size of which is of the same order as that for inner particles.

The sheet crystallization of nickel antigorite evacuated at 700°C would induce the formation of platelets. Taking into account results obtained on films (*19*, *20*, *21*), it can be supposed that the platelets are formed from tetrahedral or octahedral nuclei. All the exposed faces must be in this case (111) faces.

(*3*) *Reduction of nickel antigorite evacuated at 960°C* (*A 960–700° sample*). The reduction at 700°C of nickel antigorite previously evacuated at 960°C gives a completely reduced sample (more than 99%) after 16 hr. The nickel crystallites are larger than in the former case. Sizes and forms of these particles are heterogeneous, and they do not give any preferential orientations.

IV. Influence of Water on the Reduction

The catalyst obtained by reduction of the nickel antigorite evacuated at 700°C is more homogeneous than that obtained by direct reduction at the same temperature. It is likely that the water formed during decomposition or reduction can influence the obtained orientation.

In order to eliminate more quickly the formed water, we have directly reduced the nickel antigorite at 700°C in a dynamical system. The obtained product is more homogeneous than the one reduced in a static system, and the electron diffraction pattern obtained on each isolated sheet has twelve spots on the (220) ring of the nickel. Otherwise, if the nickel antigorite has been pressed before heating, or if the sheets are rolled, the desorption of water during heating is more difficult; when pressed or rolled samples are reduced in a dynamical system, the obtained catalysts are not homogeneous, and a mixture of orientations is observed with a majority with the (110) plane perpendicular to the electron beam. But, if we reduce the sample evacuated at 700°C with a mixture of hydrogen and water, we do not see any modification in the electron diffraction pattern obtained.

So it seems that the desorption of water formed during the decomposition of nickel antigorite is the factor that influences the orientation of nickel after reduction.

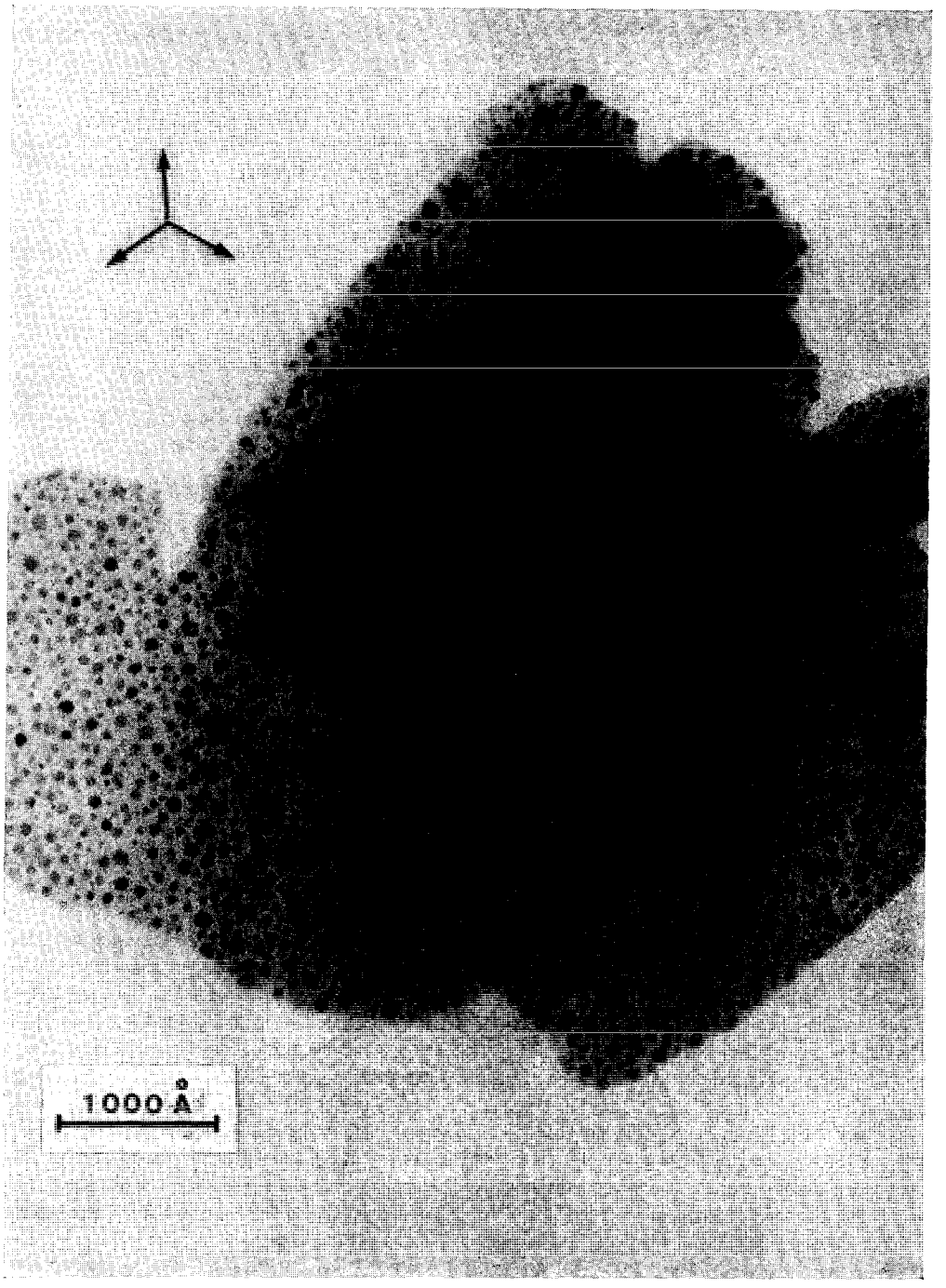

FIG. 8. Evacuated at 700 and reduced at 700°C nickel antigorite (A 700–700° sample). ×220,000.

TABLE II

MISFITS BETWEEN DISTANCES r_{hkl} OF SUPPORT AND r_{hkl} OF NICKEL IN THE CASE OF THE A ORIENTATION TYPE (110)

Misfit between distances r_{hkl} of nickel and support	Support nickel antigorite	Support nickel antigorite evacuated at 700°C
r_{111} Ni, $2r_{110}$ support	11.5%	8%
r_{220} Ni, $2r_{200}$ support	6.1%	2.5%
r_{002} Ni, r_{020} support	15%	19.4%

V. Study of Obtained Orientations

(1) Nickel. The observed orientations can be explained by an epitaxial growth of nickel on nickel antigorite during reduction. There is a reaction between a gas and a solid, and the formed product is oriented on this solid.

Two orientation types were observed, depending on the conditions of preparation: either the (110) nickel plane or the (111) nickel plane parallel to the support sheet (that is to say, parallel to the (001) plane of start nickel antigorite).

a. *(110) orientation type.* Two possibilities of nickel orientation on the (001) plane of nickel antigorite are likely:

Orientation A:

(110) Ni // (001) antigorite,
[110] Ni // [100] antigorite,
[001] Ni // [010] antigorite.

The differences between the parameters of nickel and those of start nickel antigorite and of nickel antigorite evacuated at 700°C are summarized in Table II.

An angle of 5° is observed between the [110] axis of antigorite and the [111] axis of nickel.

Orientation B:

(110) Ni // (001) antigorite,
[001] Ni // [110] antigorite,
[110] Ni // [130] antigorite.

There is an angle of 5° between the [111] axis of nickel and the [010] axis of antigorite. The misfits between the distances of nickel and those of start nickel antigorite or evacuated antigorite are summarized in Table III.

Only one orientation, A or B, is generally observed, but sometimes a pattern corresponding to the mixture of both orientations is obtained. These (110) orientation types are only observed when water was desorbed with difficulty: pressed sample, rolled sheets, direct reduction (without preliminary heating).

b. *(111) orientation type.*

Orientation A:

(111) Ni // (001) antigorite,
[110] Ni // [110] antigorite,
[011] Ni // [010] antigorite.

The angle between the [022] axis of nickel and the [110] axis of antigorite is 6°. The misfit between the distances r_{022} of Ni and $4r_{110}$ of

TABLE III

MISFITS BETWEEN DISTANCES r_{hkl} OF SUPPORT AND r_{hkl} OF NICKEL IN THE CASE OF THE B ORIENTATION TYPE (110)

Misfit between distances r_{hkl} of nickel and support	Support nickel antigorite	Support nickel antigorite evacuated at 700°C
r_{002} Ni, $2r_{110}$ support	15%	19.4%
r_{220} Ni, $2r_{130}$ support	6.1%	2.5%
r_{111} Ni, $2r_{020}$ support	11.5%	8%

antigorite is 8%. If the antigorite is evacuated at 700°C the difference is 11%.

Orientation B:

(111) Ni // (001) antigorite,
[110] Ni // [100] antigorite,
[011] Ni // [130] antigorite.

The differences between r_{110} of nickel and $2r_{200}$ of antigorite is 6.6% when the support is not heated, and 2.6% when antigorite has been evacuated at 700°C.

The difference between the A and B (111) orientations corresponds to a rotation of 30° of the [110] axis of the nickel.

In some cases (direct reduction in a dynamical system), the electron diffraction pattern has twelve spots on the (220) ring of nickel. Dark field images have been done corresponding to each of the twelve spots, and it can be observed on the images formed by electrons corresponding to two near spots that the principal axes of the crystallites are turned 30°. So this electron diffraction pattern proceeds from the superposition of the (111) orientations A and B.

In the case of the sample evacuated at 700°C before reduction, a pattern with six spots corresponding to one (111) orientation is always obtained. When the reduction is not complete (A 700–530° sample), we have previously seen that the electron diffraction pattern of the support is still visible. The spots of nickel are in the same directions of reinforcement as the spots of antigorite evacuated at 700°C. The directions of the parallel axes are those of the (111) Type A epitaxy.

(*2*) *Nickel oxide.* When the nickel antigorite is evacuated at 960°C, we have seen that NiO is obtained, with its (111) plane parallel to the (001) plane of antigorite. We have: (111) NiO // (001) antigorite, [110] NiO // [110] antigorite, and [011] NiO // [010] antigorite.

The misfit between r_{220} of NiO and $3r_{110}$ of antigorite is 3.7% and is null when the antigorite is evacuated at 700°C.

The nickel obtained by reduction of this sample is not oriented because, in this case, it seems that NiO is formed of joined small crystallites, and there is no more monocrystalline sheet for support.

Conclusions

On catalysts obtained by reduction of nickel antigorite, chemoepitaxy occurs and nickel crystallites are oriented on the silica sheets. In nickel antigorite, each plane contains only one type of atoms (Fig. 2). During the reduction, diffusion of nickel may occur between the silica sheets, and nickel platelets are formed. Depending on the reduction conditions, either (111) or (110) orientations are obtained.

When nickel antigorite is heated at 700°C before reduction at 700°C, the nickel crystallites formed have their [111] axis perpendicular to the silica sheet. We have supposed, in this case, that the initial nucleus is tetrahedral or octahedral with only (111) planes at the surface. The platelets formed from these nuclei expose (111) faces.

On the contrary, when constitution water of nickel antigorite is not evacuated before reduction, different orientations are obtained with the [110] axis perpendicular to the silica sheet. The form of nickel crystallites is less definite, but small faces are seen. We have supposed, in agreement with the work done on metallic films, that exposed faces are (110) and (111) (*19*, *21*, *22*).

In conclusion, we have succeeded in preparing supported catalysts with well-faceted nickel crystallites presenting particular faces at their surface. The catalytic activity of these catalysts for hydrogenation of ethylene was correlated with the type of crystallographic planes at the surface of nickel particles (*23*), and interesting information on the influence of the geometric factor in catalysis was obtained. Thus, the importance of the preparation of such catalysts was demonstrated.

References

1. G. Ertl, *Surf. Sci.* **7**, 309 (1967).
2. J. C. Bertolini and G. Dalmai-Imelik, *Colloq. Int. CNRS* **135**, 187 (1969).
3. G. Dalmai-Imelik and J. C. Bertolini, *CR Acad. Sci. Paris* **270C**, 1079 (1970).
4. R. E. Cunningham and A. T. Gwathmey, *Advan. Catal.* **9**, 25 (1957).

5. A. T. GWATHMEY AND R. E. CUNNINGHAM, *Advan. Catal.* **10**, 57 (1957).
6. B. LANG, R. W. JOYNER, AND G. A. SOMORJAI, *Surf. Sci.* **30**, 440 (1972).
7. H. E. GRENGA AND K. R. LAWLESS, *J. Appl. Phys.* **43**, 1508 (1972).
8. R. VAN HARDEVELD AND A. VAN MOONFORT, *Surf. Sci.* **4**, 396 (1966).
9. R. VAN HARDEVELD AND F. HARTOG, *Surf. Sci.* **15**, 189 (1969).
10. W. ROMANOWSKI, *Surf. Sci.* **18**, 373 (1969).
11. J. J. BURTON, *Catal. Rev.* **9**, 209 (1974).
12. A. MERLIN AND S. J. TEICHNER, *CR Acad. Sci. Paris* **236**, 1892 (1952).
13. G. A. MARTIN, B. IMELIK, AND M. PRETTRE, *CR Acad. Sci. Paris* **264**, 1536 (1967).
14. G. DALMAI-IMELIK, C. LECLERCQ, AND I. MUTIN, *J. Microsc.* **20**, 123 (1974).
15. R. W. G. WICKOFF, *in* "Crystal Structures" (John Wiley & Sons, Eds.), Vol. 4, 376, Interscience Publishers, (1968).
16. G. A. MARTIN, A. RENOUPREZ, G. IMELIK, AND B. IMELIK, *J. Chim. Phys.* **67**, 1149 (1970).
17. S. CAILLERE AND S. HENIN, "Minéralogie des Argiles," Masson, Paris (1963).
18. J. LONGUET-ESCARD, *Bull. Soc. Chim.* **155**, (1949).
19. Y. FUKANO AND C. M. WAYMAN, *J. Appl. Phys.* **40**, 1656 (1969).
20. J. ALLPRESS AND J. V. SANDERS, *Aust. J. Phys.* **23**, 23 (1970).
21. J. W. MATTHEWS, *Phil. Mag.* **12**, 1143 (1965).
22. S. INO, *J. Phys. Soc. Jap.* **21**, 346 (1966).
23. G. DALMAI-IMELIK, C. LECLERCQ, J. MASSARDIER, A. MAUBERT-FRANCO, AND A. ZALHOUT, *Jap. J. Appl. Phys. Suppl.* **2**, 489 (1974).